DFT study of the M segregation on MAu alloys (M = Ni, Pd, Pt) in presence of adsorbed oxygen O and O2

ARTICLE *in* CHEMICAL PHYSICS LETTERS · JANUARY 2012

Impact Factor: 1.9 · DOI: 10.1016/j.cplett.2011.11.050

2 AUTHORS:

Dhouib Adnene
University of Dammam
17 PUBLICATIONS **39** CITATIONS
SEE PROFILE

Guesmi Hazar
Pierre and Marie Curie University - Paris 6
36 PUBLICATIONS **225** CITATIONS
SEE PROFILE

Chemical Physics Letters 521 (2012) 98–103

Contents lists available at SciVerse ScienceDirect

Chemical Physics Letters

journal homepage: www.elsevier.com/locate/cplett

DFT study of the M segregation on MAu alloys (M = Ni, Pd, Pt) in presence of adsorbed oxygen O and O_2

Adnene Dhouib [a], Hazar Guesmi [b,c,*]

[a] Université de Carthage, Unité physico-chimie Moléculaire, IPEST, BP51, 2070 La Marsa, Tunisie
[b] UPMC – Université Pierre et Marie Curie, Laboratoire de Réactivité de Surface, UMR 7197, 4 Place Jussieu, 75252 Paris, France
[c] CNRS, Laboratoire de Réactivité de Surface, UMR 7197, 4 Place Jussieu, 75252 Paris, France

ARTICLE INFO

Article history:
Received 26 September 2011
In final form 21 November 2011
Available online 25 November 2011

ABSTRACT

Segregation phenomena of group 10 (M = Ni, Pd, Pt) transition-metals substituted in Au (1 1 1) surface and sub-surface layers are investigated by DFT periodic calculations in presence of adsorbed atomic and molecular oxygen. In contrast with vacuum conditions, where the metal impurities M prefer to be in the bulk of gold, in the presence of adsorbed O or O_2, the impurities mainly segregate to the surface. The analysis of oxygen adsorption trends and electronic surface structures explain the change in the local atomic arrangement which is expected to occur on the surface of alloys during reaction conditions.

1. Introduction

The desire to synthesize efficient catalysts with well-defined, controllable properties and structures at the nanometer scale has generated great interest in bimetallic nanoclusters [1–4]. Among these bimetallic systems, gold based alloys have received particular attention due to their use in a number of catalytic reactions including the direct synthesis of hydrogen peroxide from H_2 and O_2 [5,6], synthesis of vinyl acetate [7], selective hydrogenation of butadiene [8] and so forth. In the context of CO reforming, recent experiments on gold nanoparticles with different Ni contents show an improvement of the CO oxidation rate [9]. Palladium [10] and platinum [11] also emerge as good candidates for the enhancement of such reaction.

The improvement of catalytic performance of these nanoalloys mainly originates from two concepts that differentiate the bimetallic surfaces from the pure metal: the concept of 'ensemble' or strain effect from the size mismatch of the component metal atoms, and the 'ligand' effect from the hetrometallic interactions between the surface and substrate metal atoms. The former concept refers to the fact that the addition of a second metal may block certain sites that allow decreasing or eliminating the formation of undesired intermediate. Thus, specific surface ensembles are required to serve as active sites and thus enhancing the reactivity of the catalyst [7,12]. Moreover, the adsorbate-induced segregation of metal alloys under the reaction conditions, and thus the changes in local atomic composition and surface structure have been predicted and demonstrated to occur for a number of bimetallic systems [13,14]. This means that while a given bimetallic configuration may exhibit a desired property, it is important to understand whether the particular configuration is stable under the operating environment for a specific application.

In a recent Letter [15] we have demonstrated for the case of PdAu alloy that while in the absence of gases, Pd atoms have a strong tendency to substitute Au atoms in the bulk, a reversed segregation of Pd occurs in presence of a given surface atomic oxygen coverage. This tendency was also reported in the presence of CO [16] and NO [17] gases.

In this Letter we intend to investigate the effect of adsorbed oxygen, in its atomic (O) and molecular (O_2) form, on the segregation behavior of a metal impurity, from the platinum group series, alloying gold matrix.

2. Computational details

Density Functional Theory calculations were performed employing the Vienna *Ab-initio* Simulation Package [18–20]. We used the projector augmented-wave method (PAW) [21,22] and the generalized-gradient approximation (GGA) for the exchange correlation functional [23]. The energy cutoff for the plane-wave expansion was set at 415 eV.

To model the pure metallic surfaces Au(1 1 1), Pt(1 1 1), Pd(1 1 1) and Ni(1 1 1) as well as the PtAu(1 1 1), PdAu(1 1 1) and NiAu(1 1 1) surface alloys, we adopted the slab supercell approach. All the calculations presented in this work were performed on slabs containing six atomic layers representing a 3×3 supercell, separated by 15 Å of vacuum space. Adsorbed atomic and molecular oxygen were placed on one side of each slab to minimize the induced dipole effect, which is nevertheless taken into account by applying a dipole correction [24]. Spin polarized effects were included for all calculated systems. We allowed the atomic relaxation of all metallic atoms in the top four layers of the slab plus the oxygen. The bottom two layers

* Corresponding author at: UPMC – Université Pierre et Marie Curie, Laboratoire de Réactivité de Surface, UMR 7197, 4 Place Jussieu, 75252 Paris, France.
E-mail address: hazar.guesmi@upmc.fr (H. Guesmi).

0009-2614/$ - see front matter © 2011 Elsevier B.V. All rights reserved.
doi:10.1016/j.cplett.2011.11.050

were fixed at the bulk geometry positions. The final forces on the atoms were chosen to be lower than 0.01 eV/Å. The Brillouin zone integrations were performed on a Monkhorst–Pack $3 \times 3 \times 1$ *k*-point mesh. The electronic structure of the adsorption systems was analyzed through density of states (DOS) plots and Bader charge density analysis [25] with the implementation of Henkelman and co-workers [26] which allows analyzing the density issued from VASP code. The charge density analysis was made from self-consistent calculations and from projected DOS refined with a denser $11 \times 11 \times 1$ Monkhorst–Pack grid to avoid numerical noise.

The adsorption energies (E_{ads}) of atomic and molecular oxygen adsorbed on the pure metal and MAu(1 1 1) surfaces were calculated, respectively from the equations:

$$E_{ads,O} = E_{O-slab} - E_{slab} - (1/2)E_{O2} \quad (1)$$

$$E_{ads,O2} = E_{O2-slab} - E_{slab} - E_{O2} \quad (2)$$

In these equations, the first term corresponds to the energy of the adsorbate–surface superstructure and the two remaining terms correspond to the energy of the slab and of the gaseous molecular oxygen. With the use of Eqs. (1) and (2), negative values of E_{ads} mean favorable adsorption energies.

M atom (M = Ni, Pd or Pt) substituting one Au atom from the first, second, third or fourth gold layer are the four considered impurity locations in the MAu(1 1 1) alloys. We calculated the segregation energy of M impurity in gold matrix with the following equation:

Table 1
Atomic oxygen adsorption energies E_{ads} in eV, with respect to the free oxygen molecule, over pure metal M and MAu alloy (1 1 1) surfaces. $d_{(M-O)}$ is the shortest distance, in Å, between the O atom and the metal surface atom.

	Pt		Pd		Ni		Au	
	E_{ads} O	$d_{(M-O)}$	E_{ads} O	$d_{(M-O)}$	E_{ads} O	$d_{(M-O)}$	E_{ads} O	$d_{(M-O)}$
M	−1.31	1.09	−1.40	1.10	−2.64	1.06	−0.11	1.06
MAu (M *1st*-layer)	−0.51	0.99	−0.31	1.02	−1.05	0.83		
MAu (M *2nd*-layer)	−0.03	1.02	−0.04	1.03	−0.02	1.02		
MAu (M 3rd-layer)	−0.05	1.06	−0.05	1.06	−0.04	1.06		
MAu (M 4th-layer)	−0.07	1.06	−0.07	1.06	−0.08	1.06		

Table 2
O_2 adsorption energies, E_{ads} in eV and length of the O_2 bond $d_{(O-O)}$ in Å. Values in bold indicate the adsorption energies in the preferable sites.

	Site	Pt		Pd		Ni		Au	
		E_{ads} O_2	$d_{(O-O)}$	E_{ads} O_2	$d_{(O-O)}$	E_{ads} O_2	$d_{(O-O)}$	E_{ads} O_2	$d_{(O-O)}$
M	tbt	**_0.87**	1.371	_0.89	1.346	_1.54	1.391	0.26	1.32
	tfcc	_0.83	1.394	**_1.01**	1.371	**_1.83**	1.455	0.27	1.35
	thcp	_0.74	1.382	_0.95	1.369	_1.83	1.456	0.29	1.34
MAu (M *1st*-layer)	tbt	_0.22	1.336	_0.07	1.323	_0.64	1.339		
	tfcc	**_0.22**	1.356	**_0.06**	1.343	**_0.69**	1.371		
	thcp	_0.19	1.335	_0.07	1.335	_0.68	1.355		
MAu (M *2nd*-layer)	tbt	0.33	1.31	0.31	1.31	0.31	1.32		
	tfcc	0.35	1.34	0.34	1.34	0.32	1.35		
	thcp	0.37	1.33	0.35	1.33	0.36	1.34		

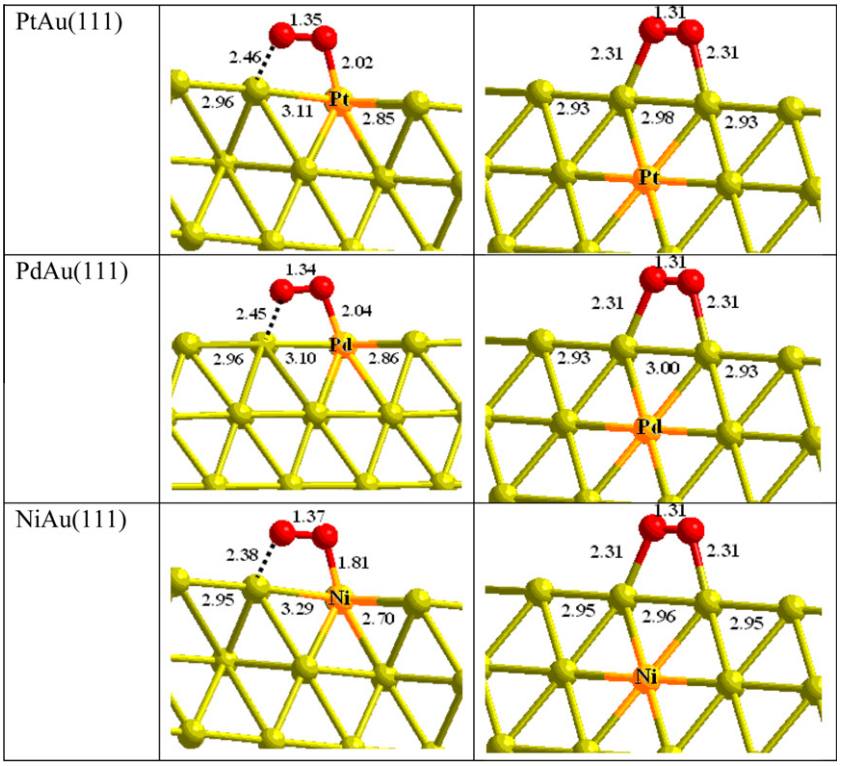

Figure 1. DFT optimized configurations of adsorbed molecular oxygen over MAu(1 1 1) surface alloys. In the left the exothermic adsorption occurs on the tfcc site in close to the M surface impurities. In the right the adsorption became endothermic once the M impurity is located in the sub-surface layer. Indicated values are in Angstrom.

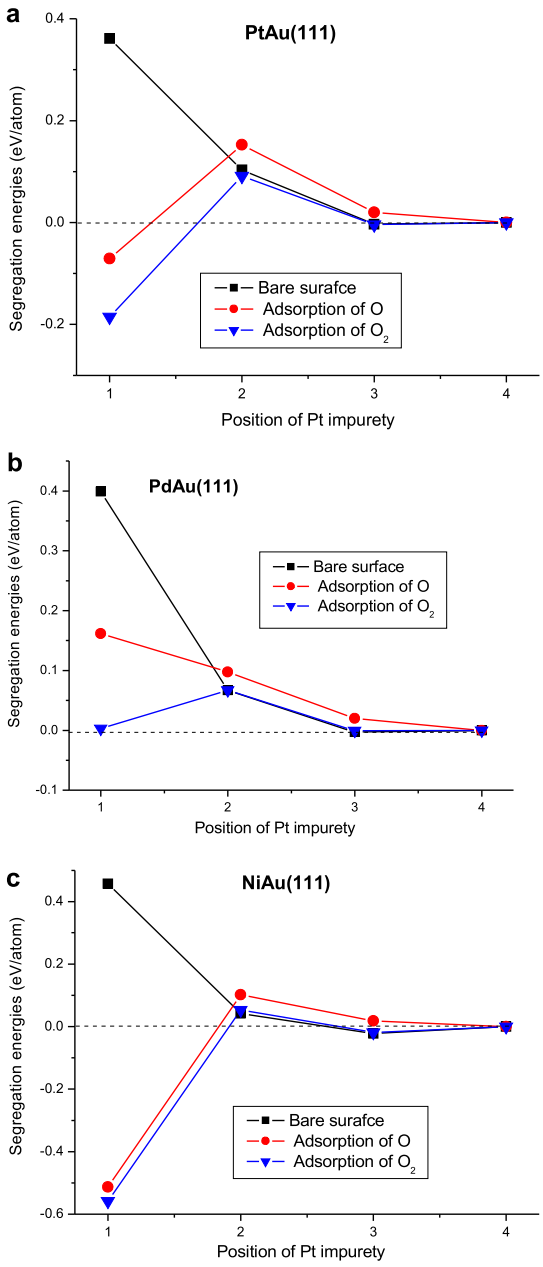

Figure 2. Evolution of the segregation energies (eV) of M impurity (M = Pt, Pd, Ni) from the gold 'bulk' (4th layer) to upper layers toward the surface in the presence and absence of oxygen.

$$E_{seg.} = [E_{MAu(M\ x\text{-layer})} - E_{MAu(M\ 4th\text{-layer})}] \quad (3)$$

where $E_{MAu(M\ x\text{-layer})}$ represents the total energy of the MAu(1 1 1) surface alloy with the M atom located in the upper xth gold layer (x = 1, 2 or 3) and $E_{MAu(M\ 4th\text{-layer})}$ represents the total energy of the MAu(1 1 1) surface alloy with the M atom located in the 4th gold layer. This latter system corresponds to a highly diluted M substituted in bulk gold matrix. The segregation energies of the systems in presence of gas were calculated taking into account the MAu alloys in the presence of adsorbed atomic or molecular oxygen; they are compared with those of the MAu systems under vaccum ('clean' MAu).

3. Results and discussion

3.1. Atomic oxygen adsorption

Atomic oxygen adsorption on closed packed transition metals (TMs) has been extensively reported [27–35]. Consistent with results of other TMs, the atomic oxygen is found to prefer the fcc hollow sites on fcc M(1 1 1), Au(1 1 1) and MAu(1 1 1): On the basal planes, oxygen is always found to occupy those sites that continue the bulk layer sequence [27–29]. On the M clean surfaces adsorption occurs with energy range of −2.64 (Ni) to −1.31 eV (Pt) with respect to half gas-phase molecular oxygen (see Table 1). These values are largely higher than the interaction energy between atomic oxygen and Au(1 1 1) surface, found to be of −0.11 eV. Surprisingly, in spite of this great energy difference the vertical O-substrate distance does not display a notable variation in all the O/TMs systems.

The affinity of oxygen atom to the platinum group instead of gold can clearly be attested by the strong adsorption energies when considering MAu(1 1 1) alloy systems including M impurity in the first surface layer. Thus, with respect to the energies, the adsorption on PdAu(1 1 1), PtAu(1 1 1) and NiAu(1 1 1) alloys, which occurs on the fcc sites close to the metal impurity, is augmented three, five and ten times, respectively from the energy obtained for pure Au(1 1 1) surface: from −0.11 to −0.31, −0.51 and −1.05 in Au *vs.* PdAu, PtAu and NiAu, respectively. This effect disappears once the impurity M is considered in the sub-surface layers of the alloy. For these particular configurations the oxygen adsorption energies became lower then on the pure gold surface, which reflect the instability of the alloy atomic configuration. On NiAu, where the oxygen interact the strongest with the surface impurity, the shorter vertical O-substrate distance of 0.84 Å is enlarged to a distance equivalent to that of O-Au (1.06 Å) when the nickel is located in the third layer of the slab. The similar behavior is noticed for the other MAu alloy systems which indicates that on gold based alloys, the oxygen atom

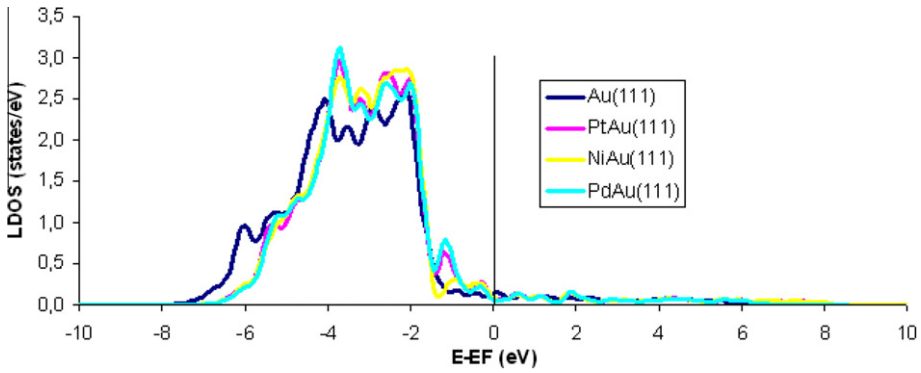

Figure 3. The local density of states (LDOSs) for the Au atom in pure Au(1 1 1) surface (dark color) and in MAu(1 1 1) alloy surfaces (light colors). (For interpretation of the references in color in this figure legend, the reader is referred to the web version of this article.)

interaction is not affected by the impurity when located as profound as the third layer of the slab.

3.2. Molecular oxygen adsorption

In Table 2 are depicted all DFT calculated adsorption energies as well as O–O bond lengths of molecular O_2 adsorbed over investigated pure and alloy metallic surfaces. Based on previous researches [30,36], three main positions for adsorbed O_2 are possible: tfcc, thcp and tbt sites. In the tfcc and thcp configurations, one of the O atoms is close to the hollow site and the second one is close to the top site of the metal. In the tbt configuration, both O atoms are close to top sites while the center of mass is places at the bridge site. The DFT optimization results of adsorbed O_2 on pure M(1 1 1) surfaces agree well with those of previous DFT calculations: tbt adsorption site on Pt(1 1 1) with E_{ads} of −0.87 eV [30,31], and tfcc adsorption configurations on Pd(1 1 1) and Ni(1 1 1) with E_{ads} of −1.01 and −1.83 eV, respectively [32]. As expected, no interaction occurs between O_2 and gold surface [35]. This result is in agreement with experimental findings reporting that oxygen does not adsorb on Au(1 1 1) at low O_2 pressure over a wide range of temperature (300–1000 K) [33,34].

For MAu(1 1 1) alloys, adsorption is found uniquely in the sites involving an M impurity. This means that once the Pd, Pt or Ni atom moves from the surface into the gold sub-layers (or into the bulk), no more interaction occurs between O_2 molecule and the alloy surface. Similarly to the case of atomic oxygen, the calculated adsorption energies of molecular O_2, adsorbed near M surface impurities, is found to increase from Pd to Ni as: PdAu(1 1 1) < PtAu(1 1 1) < NiAu (1 1 1). Former studies on alloy models show molecular oxygen adsorption energies of comparable magnitude. It shows also that in order to activate the molecular oxygen bond the catalyst should contain high index surfaces or defects generating high under-coordinated M atoms [37,38].

Although the calculated O_2 adsorption energies in the different alloy systems (Table 2) do not allow discrimination between the preferable adsorption site, the tfcc sites seem to lead to a specific configurations where the $d_{(O-O)}$ bond lengths are the largest. As illustrated by Figure 1, these bonds are already shortened in the absence of M surface impurities. In addition, the strong surface deformations ($d_{(M-Au)}$ elongation) induced by the presence of O_2, especially for the cases of NiAu(1 1 1) and PtAu(1 1 1), disappear once the impurity lives the surface (see Figure 1).

3.3. Segregation behavior

In Figure 2 are plotted the evolutions of segregation energies in alloy systems for each impurity (Pd, Pt or Ni) as a function of its position in the gold matrix. These evolutions are analyzed in presence and absence of adsorbed gas. For the three investigated alloys before adsorption i.e. under vacuum conditions, the M impurity prefers to be in the bulk of gold rather than in the surface or sub-surface layers. This is due to the smaller surface energy of gold compared to that of 10 group transition metals (experimental values are 0.64 eV/atom for Au [39], 0.86 for Pd [40], 1.03 eV/atom for Pt and 0.8 eV/atom for Ni [41]). In presence of adsorbed gas, the segregation behavior is drastically changed attesting new stable surface configurations. In fact, in presence of adsorbed O and O_2, the impurity becomes highly stable on the surface of the alloy. For PdAu(1 1 1) system, we have already reported that the surface segregation of Pd atoms, which is oxygen coverage dependant [15], is found when more than 1/3ML atomic oxygen is adsorbed on the alloy surface. In contrast, in the cases of PtAu(1 1 1) and NiAu(1 1 1) (see Figure 2a and c), as soon as one oxygen atom is adsorbed, the stability of the surface M impurities are reversed. The Ni and the Pt prefer to be on the surface of the gold and directly interact with oxygen atom. The same behavior is found for the three alloy systems in

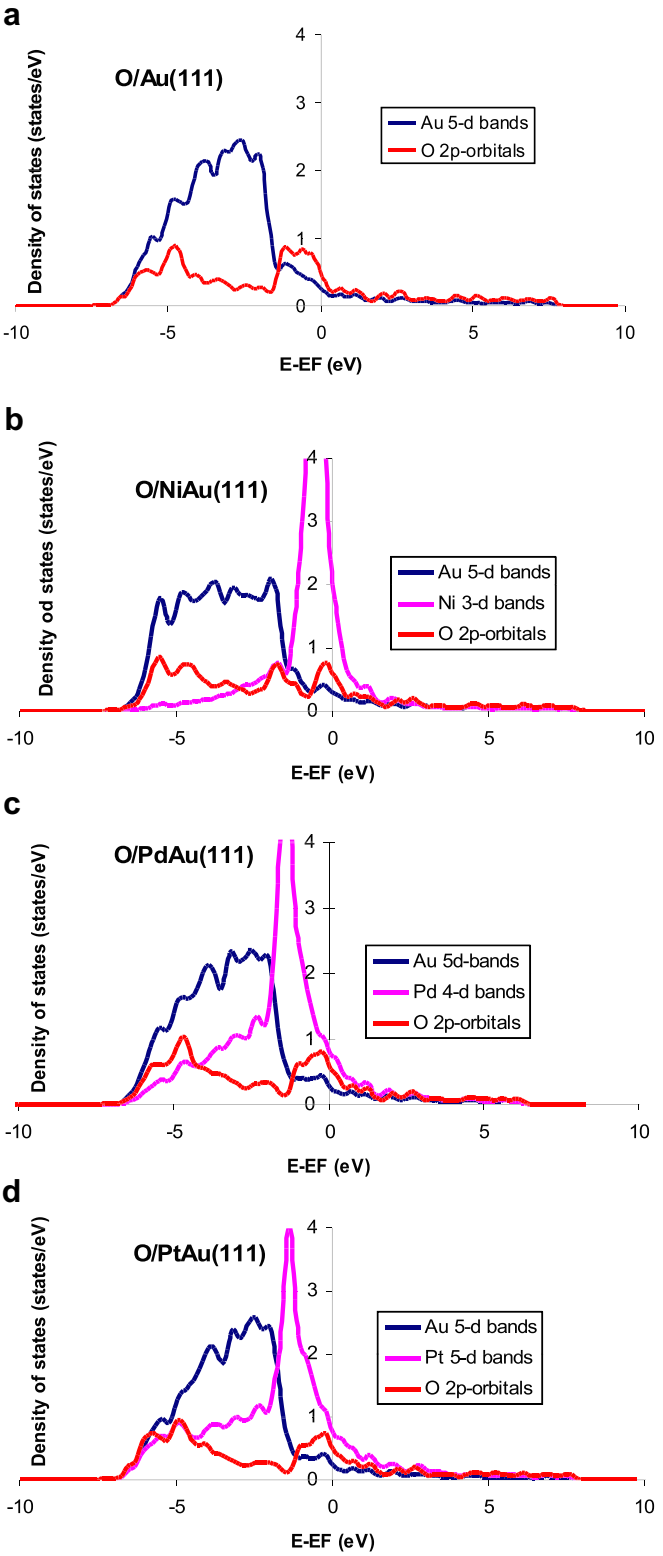

Figure 4. d-band DOSs in oxygen adsorbed systems (a) Au in pure Au(1 1 1) surface, (b) Au and Ni interacting with oxygen atom in NiAu(1 1 1), (c) Au and Pd interacting with oxygen atom in PdAu(1 1 1), (d) Au and Pt atoms interacting with oxygen in PtAu(1 1 1). The 2p orbitals for the adsorbed oxygen are indicated in red lines. (For interpretation of the references in color in this figure legend, the reader is referred to the web version of this article.)

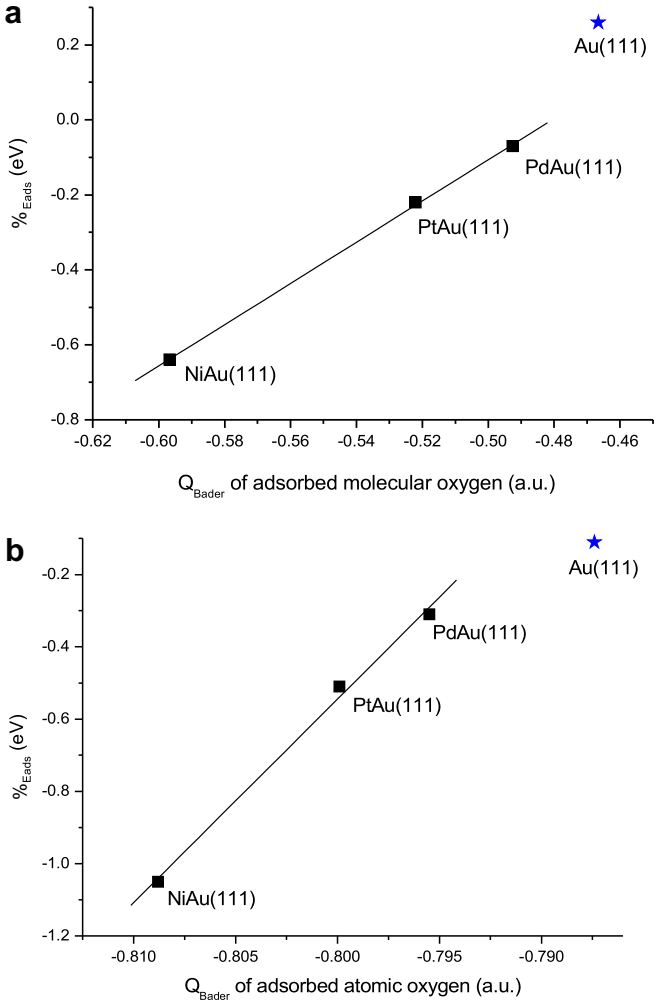

Figure 5. Evolution of oxygen Bader charges, (a) O_2 and (b) O, adsorbed on the different alloy systems as a function of calculated adsorption energies. The blue stars indicate the Bader charge of adsorbed oxygen on pure Au(1 1 1). (For interpretation of the references in color in this figure legend, the reader is referred to the web version of this article.)

presence of O_2 molecule where the effect increase in the same way as for the calculated adsorption energies i.e. Pd < Pt < Ni. Finally, as one can see form the Figure 2a–c, when the M impurity is located in the second layer of the slab, the system behaves similarly independently from the presence of molecular oxygen. The only difference is that, in presence of O_2, such impurity would probably migrate to the surface instead of into the bulk.

3.4. Electronic structure analysis

Trends in adsorption of alloys when compared to pure metals can be rationalized through the d-band model developed by Hammer and Nørskov [42,43]. The model states that the position of the d-band center relative to the Fermi level is the main parameter controlling adsorption. When an M impurity is in the gold surface layer, electronic and geometrical effects provoke an up shift in the d-center and thus oxygen adsorption increases. This can be seen in Figures 3 and 4 where the local density of states (LDOSs) for gold in Au(1 1 1) and MAu(1 1 1) surfaces before and after oxygen adsorption are plotted, respectively. Figure 3 shows how, compared to the pure Au, the d-band of Au atom, which has an M impurity as neighbor, moves close to the Fermi level. The d-band center is found to shift from −3.36 eV in pure gold to −3.09 eV in PdAu and −3.07 eV in NiAu and PtAu. The slightly high shift recorded for Ni and Pt containing alloys is in line with the high calculated adsorption energies of oxygen in these systems.

In Figure 4a, the d band of coin metal lies well bellow the Fermi level and both bonding and antibonding parts of the oxygen DOS are filled. This explains the lower interaction energy between oxygen and gold. In presence of Pt, Pd or Ni in the alloy surface (Figure 4b–d, respectively), the O–M anti-bonding states, located near the top of the M d-band around the Fermi level, are partially unoccupied, thus allowing a strong covalent bonding between the surface impurity and the oxygen atom. The same trend is found for adsorbed O_2 molecule.

To further investigate the effect of adsorbed gas on the stability of metal impurity on gold surface, we analyzed the evolution of oxygen Bader charges on the different investigated systems. Figure 5 gathers such evolution as a function of adsorption energies. As expected, the charges on oxygen atoms become more negative on going from molecular (Figure 5a) to atomic (Figure 5b) oxygen adsorbed on gold and on MAu surfaces. Compared to on pure Au(1 1 1) surface the charges of oxygen atoms increases significantly when the transition metal impurity M is substituted in the surface. These charges increase from Pd to Ni passing by Pt and an almost linear correlation is found between the calculated adsorption energies and the oxygen charges. These results show that charge transfer from the surface impurity plays an important role for the stability of the alloying system, i.e. the stability of such impurities on the based gold surface alloys in presence of reactive gas.

4. Conclusion

In conclusion, first-principles total energy calculations were carried out to study the effect of oxygen adsorption on the segregation behavior of metal impurities (M = Pt, Pd, or Ni) substituted on gold (1 1 1) surfaces. Our results show that the segregation of Platinum and Nickel, which prefer to be in the gold bulk matrix under vacuum, is completely reversed in presence of small amount of oxygen. The Pd, which segregation energy was shown to be atomic oxygen coverage dependant [15], shows high stability on the gold surface in presence of molecular oxygen. The electronic structure analysis explains the evidence of the affinity of highly diluted group 10 metals in a gold matrix to the oxygen and thus explains their surface segregation in presence of reactive gas. From these results we learn how designing specific structure in bimetallic alloys for catalytic purpose is complicated by the fact that a given surface structure might not be stable under reaction condition and that the acknowledgment of local arrangement of atoms in presence of adsorbed gas is of primary importance.

Acknowledgments

This work was performed using HPC resources from GENCI-[CCRT/CINES/IDRIS] (Grant2011-[x2011086689]). The authors thank Dr. Frederik Tielens from UPMC for the fruitful discussions.

References

[1] J. Rodriguez, Surf. Sci. Rep. 24 (1996) 223.
[2] D.P. Woodruff, The chemical physics of Solide Surfaces Alloy surfaces and Surface Alloys, Elsevier, Amsterdam, 2002. p. 10.
[3] R. Ferrando, J. Jellinek, R.L. Johnston, Chem. Rev. 108 (2008) 84.
[4] G. Mazzone, I. Rivalta, N. Russo, E. Sicilia, J. Phys. Chem. C 112 (2008) 6073.
[5] J.K. Edwards, G.J. Hutchings, Angew. Chem. Int. Ed. 47 (2008) 9192.
[6] J.K. Edwards, B. Solsona, A.F. Carley, A.A. Herzing, C.J. Kiely, G.J. Hutchings, Science 323 (2009) 1037.
[7] M. Chen, D. Kumar, C.W. Yi, D.W. Goodman, Science 10 (2005) 291.
[8] A. Hugon, Catal. 274 (2010) 239.

[9] B.O. Chandler, C.G. Long, J.D. Gilberson, C.J. Pursell, G. Vijayaraghavan, K.J. Stevenson, J. Phys. Chem. C 114 (2010) 11498.
[10] F. Gao, Y. Wang, D.W. Goodman, J. Am. Chem. Soc. 131 (2009) 5734.
[11] S. Zhou, G.S. Jackson, B. Eichhorn, Adv. Funct. Mater. 17 (2007) 3099.
[12] F. Maroun, F. Ozanam, O.M. Magnussen, R. Behm, Science 293 (2001) 1811.
[13] K.J. Andersson, F. Calle-Vallejo, J. Rossmeisl, I. Chorkendorff, J. Am. Chem. Soc 131 (2009) 2404.
[14] C.A. Menning, J.G. Chen, J. Chem. Phys. 130 (2009) 174709.
[15] H. Guesmi, C. Louis, L. Delannoy, Chem. Phys. Lett. 503 (2011) 97.
[16] V. Soto-Verdugo, H. Metiu, Surf. Sci. 601 (2007) 5332.
[17] T.V. de Bocarme, M. Moors, N. Kruse, I.S. Atanasov, M. Hou, A. Cerezo, G.D.W. Smith, Ultramicroscopy 109 (2009) 619.
[18] G. Kresse, J. Hafner, Phys. Rev. B 49 (1994) 14251.
[19] G. Kresse, J. Furthmüller, Comput. Mater. Sci. 6 (1996) 15.
[20] G. Kresse, J. Furthmüller, Phys. Rev. B 54 (1996) 11169.
[21] G. Kresse, D. Joubert, Phys. rev. B 59 (1999) 1758.
[22] P.E. Blöchl, Phys. Rev. B 50 (1994) 17953.
[23] J.P. Perdew, J.A. Chevary, S.H. Vosko, K.A. Jackson, M.R. Pederson, D.J. Singh, C. Fiolhais, Phys. Rev. B 46 (1992) 6671.
[24] J. Neugebauer, M. Scheffler, Phys. Rev. B 46 (1992) 16067.
[25] F.W. Bader, Atoms in molecules: a quantum theory, Oxford Science, Oxford, UK, 1990.
[26] E. Sanville, S.D. Kenny, R. Smith, G. Henkelman, J. Comput. Chem. 28 (2007) 899.
[27] M. Todorova, K. Reuter, M. Scheffler, J. Phys. Chem. B 108 (2004) 14477.
[28] M.V. Ganduglia-Pirovano, M. Scheffler, Phys. Rev. B 59 (1999) 15533.
[29] W.X. Li, C. Stampfl, M. Scheffler, Phys. Rev. B 65 (2002) 075407.
[30] Z. Yang, J. Wang, X. Yu, Chem. Phys. Lett. 499 (2010) 83.
[31] Y. Xu, A.V. Ruban, M. Mavrikakis, J. Am. Chem. Soc. 126 (2004) 4717.
[32] A. Eichler, F. Mittendorfer, J. Hafner, Phys. Rev. B 62–7 (2000) 4744.
[33] D.D. Eley, P.B. Moore, Surf. Sci. 76 (1978) 599.
[34] N.D.S. Canning, D. Outka, R.J. Madix, Surf. Sci. 141 (1984) 240.
[35] T. Visart de Bocarmé et al., J. Chem. Phys. 125 (2006) 054703.
[36] M. García-Mota, N. López, Phys. Chem. Chem. Phys. 13 (2011) 5790.
[37] F. Tielens, J. Andrés, T-D. Chau, T. Visart de Bocarmé, N. Kruse, P. Geerlings, Chem. Phys. Lett. 421 (2006) 433.
[38] F. Tielens, J. Andrés, M. Van Brussel, C. Buess-Herman, P. Geerlings, J. Phys. Chem. B. 109 (2005) 7624.
[39] W.R. Tyson, W.A. Miller, Surf. Sci. 62 (1) (1977) 267.
[40] L.Z. Mezey, J. Giber, Jpn. J. Appl. Phys. 21 (1982) 1569.
[41] L. Vitos, A.V. Ruban, H.L. Skriver, J. Kollár, Surf. Sci. 411 (1998) 186.
[42] B. Hammer, J. Nørskov, Surf. Sci. 343 (1995) 211.
[43] B. Hammer, J. Nørskov, Nature 376 (1996) 238.